Pergamon

PII: S0191–8141(98)00013–3

Journal of Structural Geology, Vol. 20, No. 6, pp. 799 to 818, 1998

0191-8141/98 $19.00 + 0.00

Orogen-parallel strike-slip faults bordering metamorphic core complexes: the Salzach–Enns fault zone in the Eastern Alps, Austria

XIANDA WANG and FRANZ NEUBAUER

Department of Geology and Paleontology, University of Salzburg, Hellbrunner Straße 34, A-5020 Salzburg, Austria

(*Received* 27 *May* 1997; *accepted in revised form* 9 *February* 1998)

Abstract—The approximately ENE-trending Salzach–Enns fault (Eastern Alps) contributed to late-stage exhumation of the Tauern metamorphic core complex in response to oblique convergence of European and Adriatic plates. Six stages of kinematic evolution with early ductile and later brittle deformational structures were recognized as follows: (1) Initial ductile deformation is represented by a combination of sinistral shear-dominated noncoaxial strain and coaxial strain. (2) Early brittle sinistral strike-slip is combined with a pure shear deformation and represents roughly N–S contraction. It is followed by (3) sinistral strike-slip and (4). ca. N–S extension due to normal-slip striations. (5) Subsequent N–S compression resulted in counterclockwise rotation of the maximum principal stress from NE to NW and led to final dextral strike-slip displacements along the Salzach–Enns fault.

The exhumation of the Tauern Window was accommodated by dip-slip on the fault plane at shallow levels and coaxial flattening at deeper structural levels. Brittle sinistral faults at shallow structural levels produced a larger amount of strike-slip displacement than ductile shear zones at the deeper structural levels, which is explained as a scissors-like movement and which resulted in the eastward tilting of the Tauern Window. © 1998 Elsevier Science Ltd. All rights reserved

INTRODUCTION

It is believed that most orogenic belts around the world are the product of oblique plate convergence (e.g. Woodcock, 1986). Transpression due to oblique convergence is often partitioned into orogen-perpendicular contraction, orogen-parallel extension and strike-slip displacement (e.g. Ratschbacher *et al*., 1989, 1991; Holdsworth and Strachan, 1991; Manning and Bartley, 1994; Tikoff and Teyssier, 1994). Extensional structures responsible for unroofing and exhumation of metamorphic complexes and the development of metamorphic domes during late-orogenic, overall contractional stages have been investigated over the past decade (e.g. Coney, 1980; Malavielle, 1987; Dewey, 1988; Lister and Davis, 1989; Platt, 1993; Neubauer *et al*., 1995). Major strike-slip faults along the margins of metamorphic domes are likely to play a significant role in the exhumation process of metamorphic domes. Some major strike-slip faults experienced significant vertical movement and juxtapose rocks initially metamorphosed at different crustal levels (Suggate, 1963; Ichikawa, 1980; Peltzer *et al*., 1985).

The present-day tectonic framework of the Tauern Window, Eastern Alps, is characterized by Neogene east–west extension subparallel to the orogen (e.g. Ratschbacher *et al*., 1989, 1991). This late-orogenic extension resulted in top-to-the-west low angle normal shear along the western margin of the Tauern Window (Selverstone, 1985, 1988; Behrmann, 1988) and top-to-the-east low-angle normal shear along its eastern margin (Genser and Neubauer, 1989). Simultaneously, strike-slip fault zones formed parallel to the strike of orogen (Neubauer and Genser, 1990; Ratschbacher *et al*., 1991). Petrologic and geochronological data were used to reconstruct the exhumation history of units exposed in the Tauern window (e.g. Selverstone, 1985, 1988; Droop, 1985; Staufenberg, 1987). In combination with structural observations these indicate that orogen-parallel extension occurred after the pressure peak of metamorphism and caused exhumation of the previously buried Penninic oceanic and underlying continental lithosphere within the metamorphic dome (Selverstone, 1985, 1988; Ratschbacher *et al*., 1989). Various structural evolution models for exhumation of the Tauern window during the Tertiary have been proposed (e.g. Lammerer, 1988; Genser and Neubauer, 1989; Ratschbacher *et al*., 1991). Most models emphasize a significant contribution of displacement along the Salzach–Enns strike-slip fault to the exhumation of the Tauern window.

In this study, the ductile and brittle structures along the Salzach–Enns fault are described in detail. The results are used to constrain the kinematics and structural history of the Salzach–Enns fault and to examine existing structural models for strike-slip faults bordering metamorphic core complexes.

STRUCTURE ALONG THE SALZACH–ENNS FAULT

The Salzach–Enns fault trends ENE along the middle and eastern sections of the northern margin

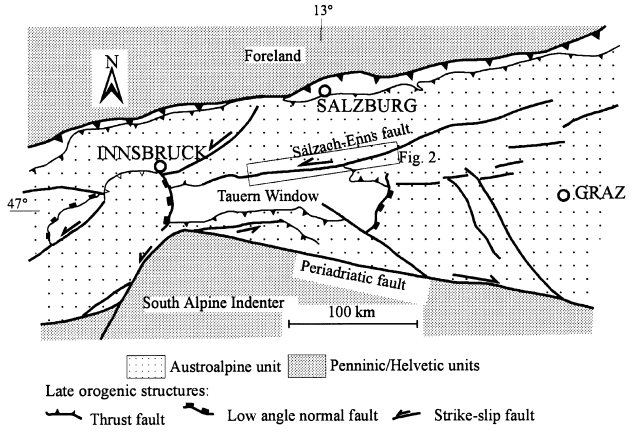

Fig. 1. Simplified structural map with late stage orogenic structures of the Eastern Alps and location of the Salzach–Enns fault. The rectangle locates Fig. 2.

of the Tauern window and extends at least 100 km further eastwards (maximum: approximately 300 km for the Salzach–Enns–Puchberg–Mariazell fault; e.g. Ratschbacher *et al*., 1991; Linzer *et al*., 1997; Nemes *et al*., 1995) (Fig. 1).

The northern side of the fault exposes the Lower Austroalpine unit west of Mittersill, mainly represented by black quartz phyllite, and slate-phyllites and intercalations black quartzitic rocks of the Upper Austroalpine unit (Graywacke zone) east of Mittersill (Fig. 2). The Lower and Upper Austroalpine units are part of the Austroalpine Nappe Complex representing the hangingwall continental plate during Tertiary continental collision. In contrast, the southern side of the Salzach–Enns fault includes various rocks of the Penninic and Lower Austroalpine units (Fig. 2). From west to east, Penninic units comprise Paleozoic metasedimentary units and parautochthonous basement (Frisch, 1980) west of Mittersill, and Mesozoic rocks between Mittersill and Wagrain, mainly calcitic schists, black phyllites and marbles of the Nordrahmenzone. Thus this segment of the Salzach–Enns fault juxtaposes the Austroalpine nappe complex that is part of the Adriatic plate against the Penninic nappes that represent outliers of the European continental margin and the former oceanic basin to the south of it. The latter were subducted beneath the Adriatic plate during the Tertiary continent–continent collision (e.g. Frisch 1979; Kruhl, 1993; Fig. 1). West of Mittersill, the Salzach–Enns fault virtually disappears, and is likely replaced by a sequence of NE-trending sinistral steep shear zones inside the western Tauern Window (e.g. Behrmann and Frisch, 1990). The Salzach–Enns fault is not an ideal planar surface but forms an array of minor faults, which combine and anastomose to form a broad fault zone. In general, the Salzach–Enns fault zone trends ENE and dips steeply north, parallel to

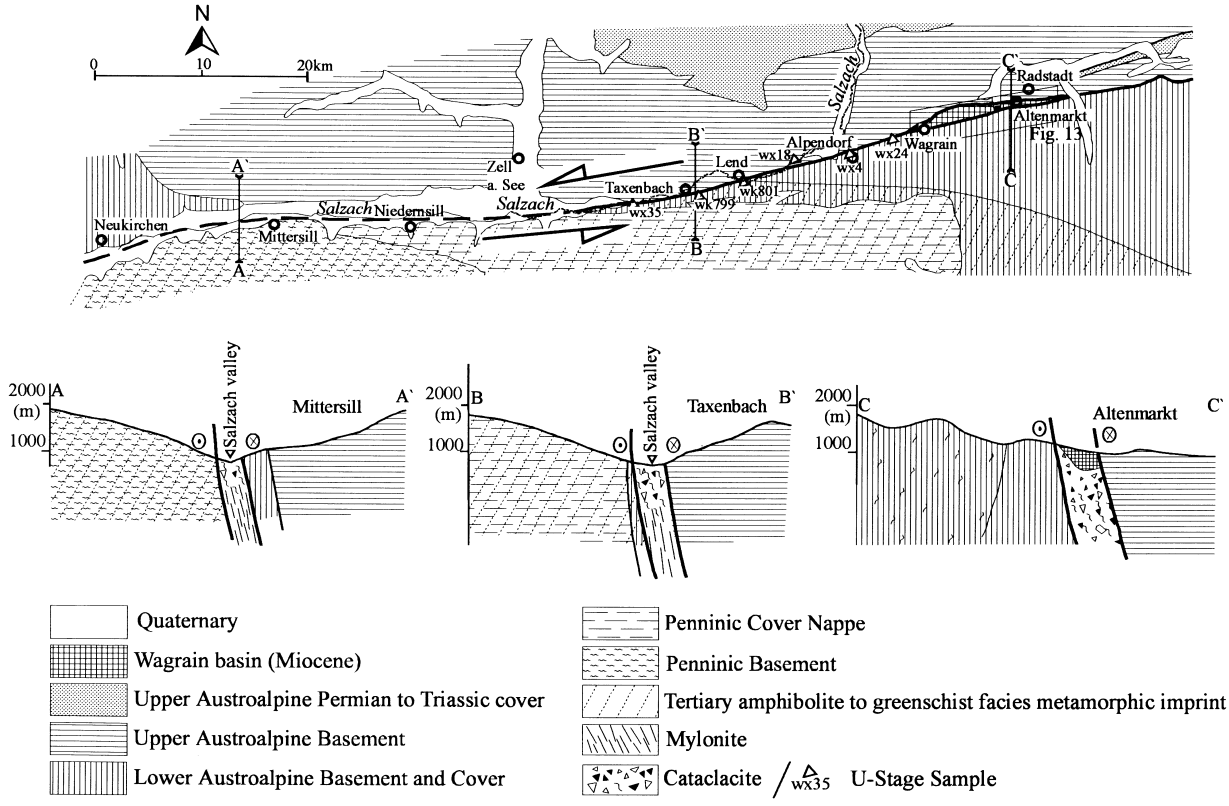

Fig. 2. Simplified geological map of the Salzach–Enns fault zone. A–A′, B–B′ and C–C′ are cross sections through western, middle and eastern sectors of the investigated segment of the Salzach–Enns fault. From west to east the structural units of the southern wall of the fault are composed of Penninic basement, the Penninic cover and Lower Austroalpine units, the structural units of the northern wall are the Lower and the Upper Austroalpine units. Location of Fig. 12 outlined by quadrilateral box.

the dip of sequences exposed on both sides of the fault.

The Penninic units of the Tauern Window were subject to Tertiary metamorphism up to amphibolite facies conditions in central parts of the window, and greenschist facies conditions along its margins (for data compilation, see Genser *et al.*, 1996). Post-peak cooling, decompression and exhumation started at ca. 30 Ma. Internal Austroalpine units were metamorphosed during the Cretaceous and cooled beneath 300°C before the Tertiary. These relationships resulted in a marked contrast in the Tertiary metamorphic grade between Penninic units exposed within the Tauern Window and surrounding Austroalpine units.

Between Wagrain and Altenmarkt a left-stepping bent segment of the Salzach–Enns fault (Fig. 2) is associated with the narrow Miocene coal-bearing Wagrain basin (Fig. 2) (Weber and Weiss, 1983; Exner, 1996). The sedimentary sequence includes a basal conglomerate covered by alternation of conglomerates and micaceous sandstones, and fine-grained sandstones, mudstones and shales at the top (Trauth, 1925). This non-metamorphic sequence is Miocene in age (Exner, 1996, and references cited therein).

STUDY AREA AND METHODS

We thoroughly investigated structures of 40 stations between Neukirchen and Radstadt extending over more than 120 km along the Salzach–Enns fault zone (Fig. 2). A succession of ductile, ductile–brittle and brittle deformation structures was observed. We examined the character of associated transected folds, crenulations and other ductile structures in light of the approaches outlined by Sanderson and Marchini (1983), Simpson and Schmid (1983), Hanmer and Passchier (1991), Treagus and Treagus (1992) and Wenk and Christie (1991). We also examined the microstructures of calcite mylonite with methods described by, e.g. Rutter *et al.* (1994), Schmid *et al.* (1987), Burkhard (1993), Lister and Williams (1979) and Wenk *et al.* (1987), in order to determine the strain geometry and sense of shear. Furthermore, we collected slickensides and striation lineations for analysis of paleostress fields formed during a succession of brittle deformation stages.

The determination of brittle deformation sequences during the field survey referred to displacement criteria in brittle faults (e.g. Petit, 1987; Gamond, 1983, 1987). Data sets of slickensides and striae were evaluated using current graphic and numerical techniques in combination with independent field criteria (e.g. Marrett and Allmendinger, 1990; Armijo *et al.*, 1982). A computer program provided by Stapel and Moeys (1994) following the approach proposed by Angelier (1979) was used to analyze multistage tensors combined with field observations.

DEFORMATION STRUCTURES

S–C fabrics

S–C fabrics are common within metapelitic and calcareous schists of the middle and western sectors of the Salzach–Enns fault (Fig. 3a, b), both *S* and *C* surfaces here recorded as deformation D_1 along the fault. The *S*-surfaces are usually represented by preferred orientations of minerals. The *C*-surfaces are simple narrow seams. The *C*-surfaces always dip towards the N and intersect the NNE-dipping *S*-surface at a low angle, while fault planes are parallel to the *C*-surfaces of sequences. In many cases, the *S*-surfaces represent the original schistosity resulting from earlier deformations within the interior of the Tauern Window (Bickle and Hawkesworth, 1978; Kurz *et al.*, 1996).

In the study area, the *C*-surfaces appear as two types: one is subvertical at a low angle to the dip of the fault surfaces. Lineations on *S*-surfaces are subhorizontal. This geometry indicates sinistral strike-slip sense (Fig. 3a). The other set of *C*-surfaces dips moderately to gently to south or north, and, is indicative of a reverse displacement along steep-dipping fault planes (Fig. 3b).

Crenulation lineations and transected folds

Crenulation lineations are common along the Salzach–Enns fault zone in schists and phyllites. In general, these crenulation lineations consistently plunge gently to the WNW (Fig. 4a). The crenulation lineations deform metamorphic minerals (Fig. 3e) and postdate, therefore, peak metamorphic conditions.

The crenulation lineations are commonly associated with transected folds parallel to intersection lineations of foliations (Fig. 4a), although there is only a slight difference in plunge directions between crenulation lineations and fold axes (Fig. 4) (e.g. Stringer and Treagus, 1980).

Within the Salzach–Enns fault zone numerous strongly non-cylindrical, centimetre- to metre-scale transected folds occur in phyllites. These are commonly tight folds with a gently to steeply dipping random orientation of axial planes. Fold hinges are slightly curved and plunge gently to the east or west (Fig. 4c). In some cases, these folds are arranged en échelon along the strike of the Salzach–Enns fault. Their hinge lines are obliquely intersected by crenulation lineations in a clockwise sense of about 8° with regard to the fold axis (Fig. 4a), and both of them intersect the strike of the Salzach–Enns fault in a clockwise sense of about 20–25°. Such transected folds are believed to derive from rotation and tightening of early folds formed obliquely to the strike-slip shear zone (e.g. Sanderson and Marchini, 1984). A sinistral transpression should be responsible for a clockwise transection (e.g. Soper and Hutton, 1984; Woodcock

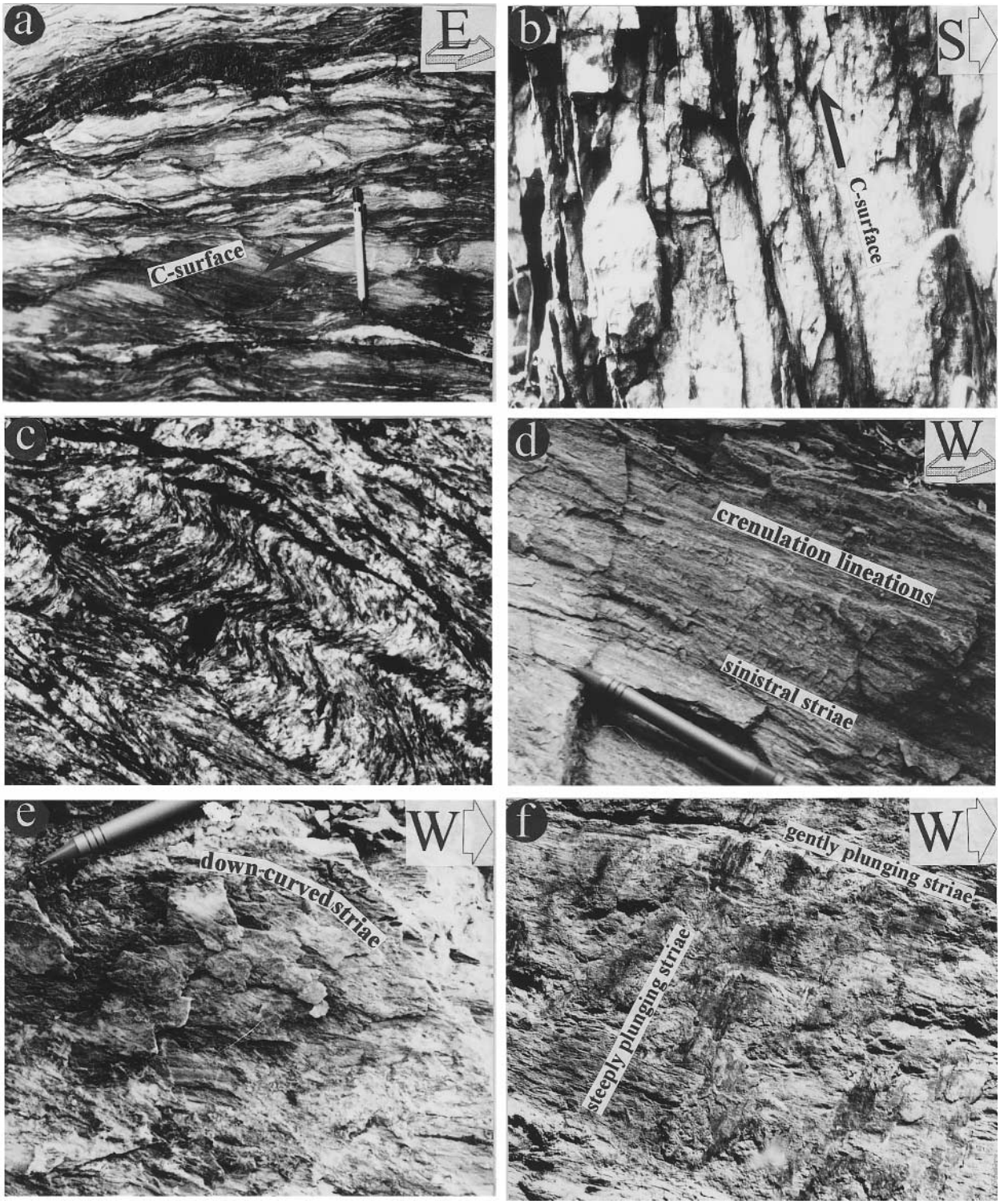

Fig. 3. Structures and microfabrics along the Salzach–Enns fault. (a) Typical *S–C* fabric within schists and phyllites of Lower Austroalpine units to the southeast of Taxenbach, middle part of the Salzach–Enns fault, which documents sinistral shear along the steep Salzach–Enns fault. (b) *S–C* fabric developed in the steeply dipping Penninic schist southwest of Taxenbach, which documents reverse displacement of the Penninic unit. (c) Crenulations in schists close to Niedernsill, which deformed an earlier foliation. Length of the photograph 1 mm. (d) Relationship between crenulations and striations. Striations indicate sinistral displacement and show continuous development linking with the crenulations at their right ends and parallel to them. Both lineations gently plunge to the west (east of Alpendorf village, middle part of the Salzach–Enns fault). (e) Sinistral shear striations which curve down westwards (east of Lend village). (f) Overprint relationships of two sets of striations with different plunge directions in the Niedernsill valley: Gently plunging striations document sinistral strike-slip displacement; steeply plunging striations document dip-slip. The latter overprint the gently plunging striations. For locations, see Fig. 2.

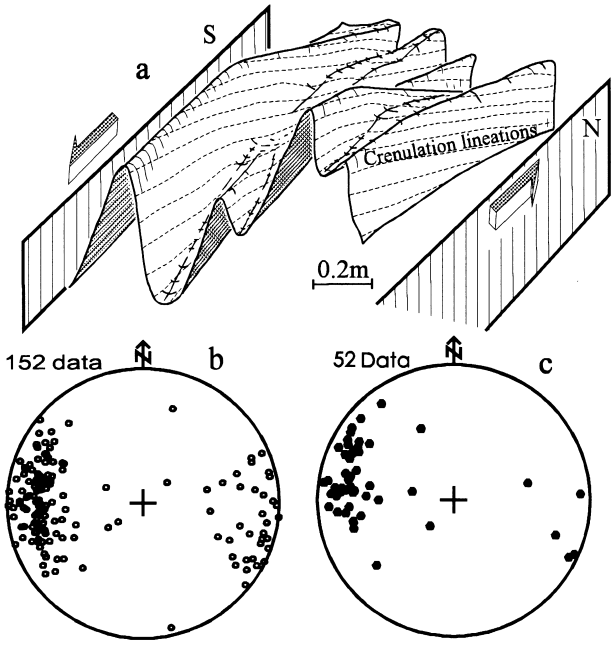

Fig. 4. Transected folds associated with the Salzach–Enns fault. (a) Shape of the folds and relationship between folds and crenulations in the Salzach–Enns fault zone. Legume-like folds (according to Ramsay and Huber, 1987) with gently plunging hinges at low angles to the general displacement direction developed in the fault zone. The folds are transected by the crenulation in a clockwise sense, which signifies sinistral transpression. (b) Stereographic projection of the axes of transected folds within the fault zone. Axes have general WNW resp. ESE plunge, oblique to the ENE trend of the fault zone. (c) Stereographic projection of the crenulation lineations, displaying an overall gentle plunge towards WNW. (b, c) Lower hemisphere, equal-area projections.

et al., 1988). In sinistral transpression, early folds are sinistrally rotated, and later cleavages are superimposed in a clockwise sense (e.g. Soper 1986; Treagus and Treagus, 1992). Continued transpression might have rotated the transected folds and crenulation lineations to orientations subparallel to the fault. Therefore, gentle E and W plunge of both the crenulation lineations and fold axes and a clockwise transection indicate a NNE–SSW oblique convergence along the Salzach–Enns fault zone.

Calcite mylonites

Microfabrics and patterns of preferred crystallographic orientation in calcite mylonites are sensitive to final stages of deformation (e.g. Lister and Williams, 1979). Therefore, the micro-fabrics and lattice-preferred orientation patterns of calcite observed in the Salzach–Enns fault zone document the kinematic character of the post-collisional Salzach–Enns faulting event rather than that of previous thrusting (Bickle and Hawkesworth, 1978; Kurz *et al.*, 1996). Calcite mylonites can be found in most locations, and these are treated as significant evidence of early ductile deformation at deeper structural levels of the fault. Dependent upon the grain size of protoliths, the microstructures of calcitic rocks in the Salzach–Enns fault vary from twinning in otherwise less deformed rocks to mylonization and ultra-mylonization.

In relatively coarse-grained carbonate rocks, calcite mylonite exhibits distinct preferred orientations of elongated twinned calcite grains (Fig. 5a). These calcite grains usually are lensoid with constricted ends. Their aspect ratio varies from 6 to 8. These microstructural characteristics reflect deformation by twinning and intracrystalline glide. With the exception of specimen WX18CC, *c*-axis textures of the calcite mylonites are dominated by two or three maxima distributed at or near to the periphery of the diagram (Fig. 6) with an angle of 15°–25° between the maximum and the foliation pole. *c*-Axis textures of specimens WK799cc, WX4cc and WX24cc are of orthorhombic symmetry with respect to two symmetry planes that are 15°–25° inclined to the foliation. In *c*-axis textures of WX35cc and WK801cc the angle is less, about 10°. Overall, the *c*-axis fabrics show general patterns interpreted to reflect pure shear strain progressive deformation under relatively low-grade conditions (ca. 300–400°C; Schmid *et al.*, 1987; Wenk *et al.*, 1987). The orthorhombic symmetry of the *c*-axis indicates approximate N–S flattening.

Specimen WX18CC (Fig. 6) represents a thin calcitic vein within quartz schist. Its single *c*-axis maximum is deflected 15° from the pole to the foliation in a counter-clockwise sense towards the shortening direction and against the imposed sense of shear that resulted from e-twinning. This indicates therefore a subhorizontal sinistral strike-slip component in about a E–W direction. In general noncoaxial flow, the angle between the *c*-axis maximum and the pole is smaller than that developed in simple shear flow regimes (normally about 30°). Wenk *et al.* (1987) argued that the angle between the *c*-axis maximum and the pole to the foliation is not a function of increasing strain but rather of an increasing components of pure shear in non-coaxial flow. Specimen WX18cc therefore indicates general non-coaxial progressive deformation conditions.

Calcite twinning commonly develops in coarse-grained rocks. Most calcite twins show moderately thick to thin and straight lamellae (Fig. 5a) similar to the geometric types I–II described by Burkhard (1993). This geometry of calcite twins is interpreted to correspond to formation at low temperatures of ca. 150–300°C or lower. Furthermore, the majority of grains displays only one set of e-twins (Fig. 4), which can be related to a dominant component of simple shear (Schmid *et al.*, 1987), indicating E–W sinistral shear. Alternatively, the conjugate twins observed in a minority of grains may represent the coaxial component of general non-coaxial progressive deformation (Schmid *et al.*, 1980).

There are two types of ultra-mylonites in fine-grained calcite rocks. One is associated with a large

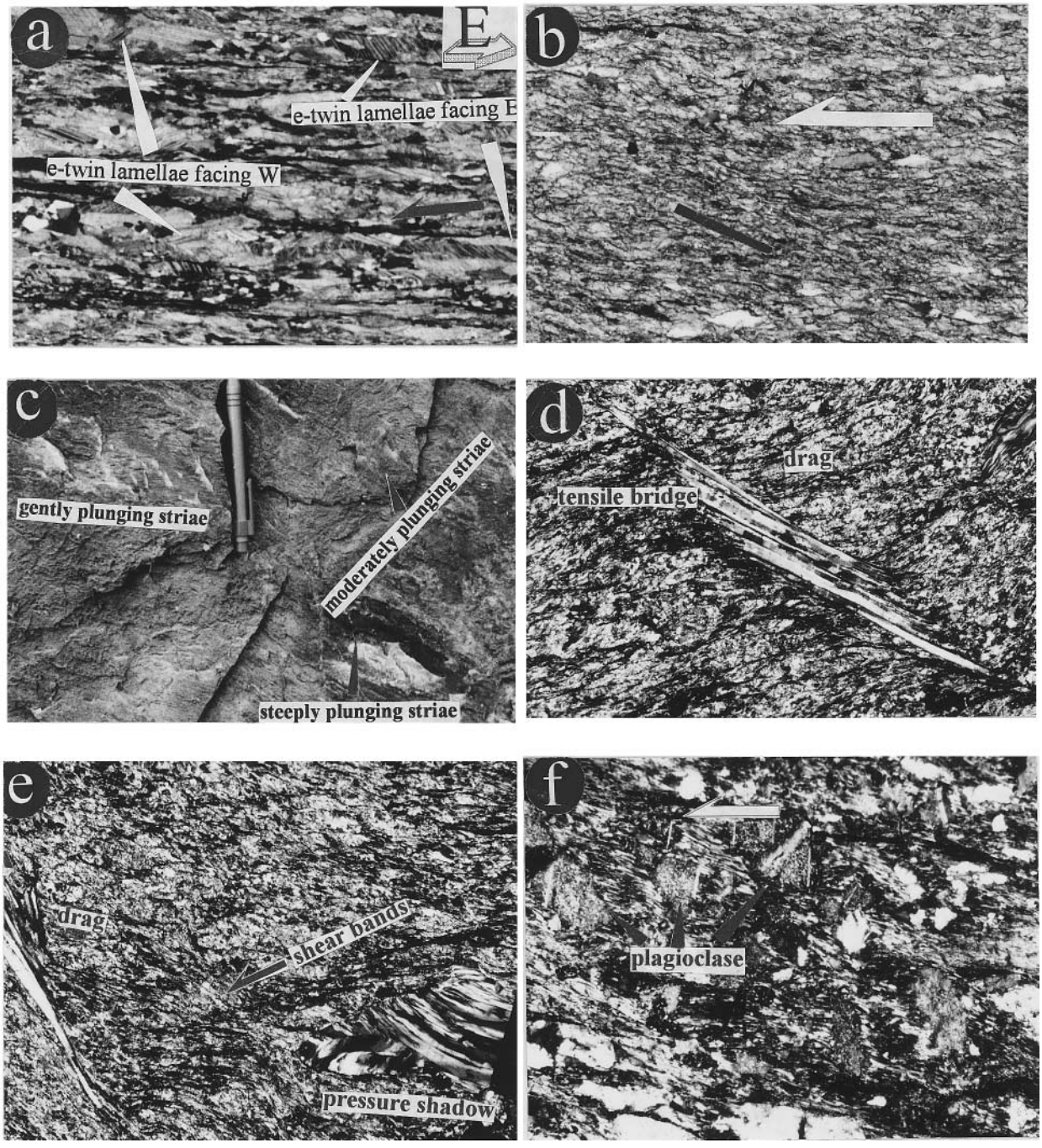

Fig. 5. Structures and microfabrics along the Salzach–Enns fault. (a) Calcite mylonite: Two sets of twins with different orientations. The lamellae are moderately thick to thin and straight. The main set of e-twins indicates ductile sinistral shearing. Length of the photograph 3.8 mm. Crossed polarizers. (b) Calcite ultra-mylonite: Black bar indicates the array of elongated grains and subgrains; white arrow indicates the shear sense of shear bands. Length of photograph 1 mm. Crossed polarizers. (c) Striations with three different plunging directions represent three stages of movement along the Salzach–Enns fault (S of Alpendorf). Moderately plunging striations represent reverse westward-slip, gently plunging striations sinistral strike-slip, and steeply plunging striations represent dip-slip displacement, respectively. (d) Tensile bridge structure displaying the micro-fabrics of main striations. Tensile bridge and schistosity drag structures show ductile–brittle fracture deformation indicating sense of displacement (S of Wagrain). Quartz fibres constitute striations and steps at mesoscopic scale. Length of photograph is 3.8 mm. Crossed polarizers. (e) Ductile shear bands and displacement-controlled strain shadows of pyrite document sinistral strike-slip, tensile bridge structures representing R' fracture with respect to ductile–brittle shear bands and drag structures indicates dextral slip (S of Wagrain). Length of photograph 3.8 mm. Crossed polarizers. (f) Porphyroclastic plagioclase with an array of dominoes and asymmetric strain shadows within Penninic basement gneiss in the Salzach–Enns fault zone, indicating brittle–ductile sinistral shearing. Length of the photographs 3.8 mm. Crossed polarizers. Location S of Taxenbach.

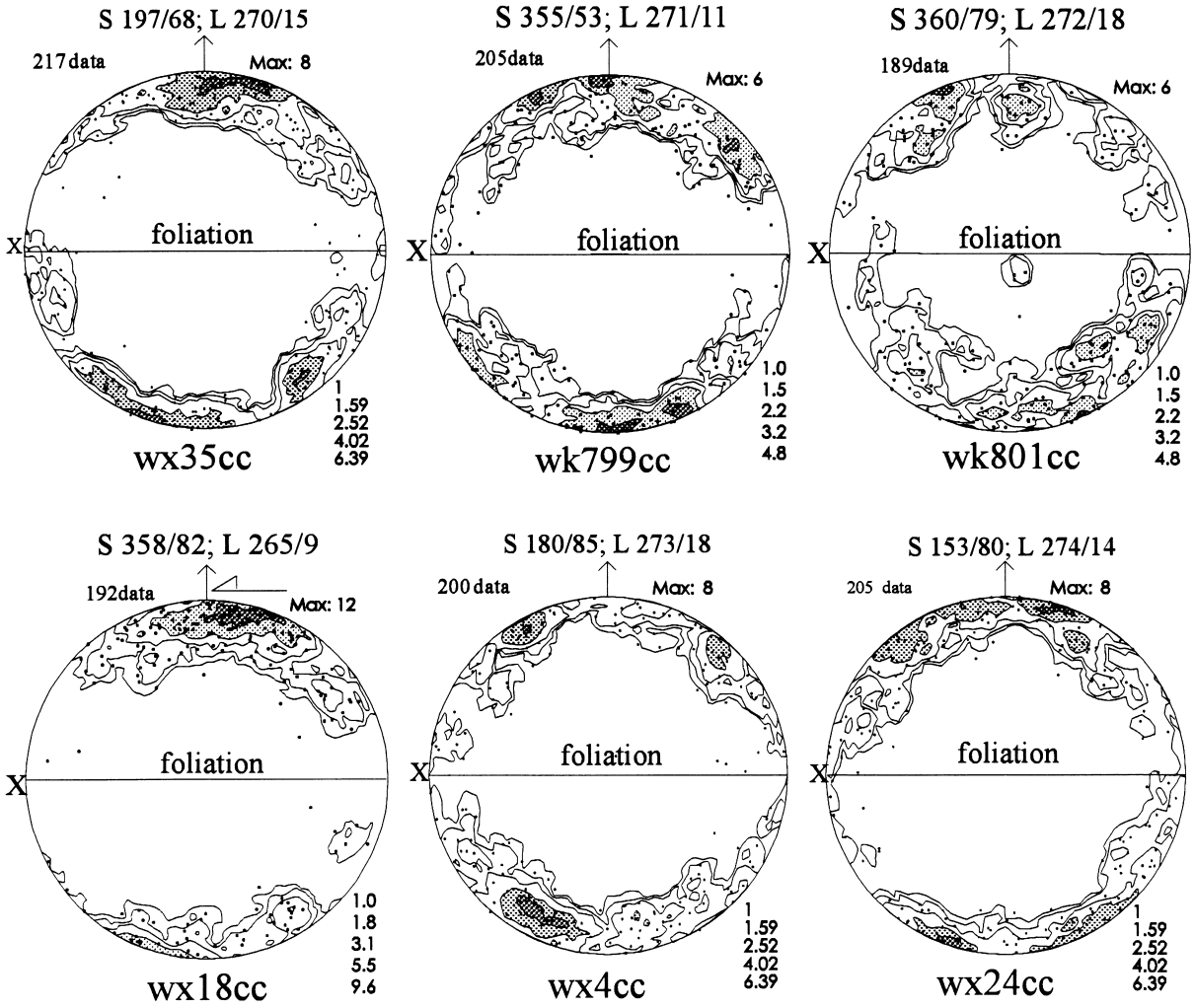

Fig. 6. Calcite *c*-axis textures: Values at the right margin of each diagram are multiples of random distributions for the areas bordered by isolines. Black and gray indicate areas of *c*-axis maximum. For explanation see text. Locations of samples are shown on Fig. 2.

number of twin lamellae. The long axes of grains in this calcite ultra-mylonite reach about 200 μm in length and their aspect ratio exceeds 1:10, showing a large amount of strain. The other calcite ultramylonite does not show twins or recovery fabrics around grain boundaries (Fig. 5b). The untwinned grain size within this ultramylonite is about 15–20 μm and aspect ratios are about 1:3.5. Many fine-grained calcite grains display a well developed preferred crystallographic orientation consistent with a sinistral sense of shear. These features are likely related to the regime of intracrystalline plastic flow. Both types of ultramylonite appear to have formed during the same structural period and within the same pressure–temperature conditions along the Salzach–Enns fault zone. The various calcite ductile structures can be explained to be result of various deformation mechanisms that contributed to deformation of the carbonates differing in grain sizes during the same tectonic event (Busch and van der Pluijm, 1995).

Semi-brittle and brittle deformation structures

Slickensides and striae are the most prominent brittle structures along the Salzach–Enns fault zone. In the field survey, the slickensides and striae can be clearly divided into a succession of kinematic stages of fault evolution, following criteria described by Hobbs *et al.* (1976), Gamond (1987) and Petit (1987). The majority of slickensides with subhorizontal striae trends ENE, a minority SSE. The first set of slickensides predominately dips to the NNW and bears either dip-slip or strike-slip striae, only few of which sharing both striae. Three differently plunging striae can be distinguished: (1) The first set of striae (D_2 and D_3) is developed best. They gently plunge to the west and sometimes curve downwards and display a sinistral sense of movement (Fig. 3e). They are parallel with crenulation lineations and seem to succeed the formation of early crenulation lineations (Fig. 5f). This implies that the brittle sinistral strike-slip postdates ductile sinistral shear represented by the crenulation

lineations. (2) In nearly all cases where both sets appear on the same slickensides, the set of sinistral strike-slip striae is overprinted by steeply plunging striations (Fig. 3f) or occur as the down-curving part of these (Fig. 3e & f). The youngest (D_4) striae show normal sense of slip. (3) The last set of striae (D_5) is less common and includes gently E–W plunging, dextral shear sets and gently N–S plunging, sinistral shear sets, clearly display dextral sense of displacement.

The slickensides and striae in the Salzach–Enns fault zone commonly display semi-brittle deformation features. On the outcrop-scale, striation-associated drag structures formed where slickensides obliquely intersect schistosity planes. On the micro-scale, schistosity planes bend into fracture seams and exhibit drag structures. Arrays of en échelon crystal fibres associated with striae and accretion steps (Norris and Barron, 1968) grew in domino-like opening domains (Fig. 5d), which originated from overstepping tensional fractures with the same attitude as P fractures (tensile bridge structures according to Gamond, 1987). These drag structures and tensile bridge structures were used as criteria to determine the sense of shear.

Microstructures in metapelites also indicate conjugate shearing in the transition of ductile to brittle deformation (Fig. 5e). Weakly developed *S*–*C* fabrics and pressure fringes with displacement-controlled fibres around euhedral pyrite (Hanmer and Passchier, 1991), define sinistral shear nearly parallel to the bulk shear direction. Tensile bridge structures define a dextral shear fracture, which represents a *R*′ fracture oriented at a large angle to the schistosity planes. The obtuse bisectrix between *C*-surfaces and *R*′ fractures indicate, therefore, the direction of the principal axis of stress. Meanwhile, the *S*-surface marks the finite flattening plane that resulted from the partitioning of deformation (Ramsay and Graham, 1970). On the other hand, arrays of dominoes of cataclastic feldspars in carbonate-bearing arkosic schist indicate sinistral brittle–ductile shear parallel to the strike of the Salzach–Enns fault zone (Fig. 5f).

From west to east, the deformation style changes from dominant ductile structures in the west to dominantly brittle structures in the east. On the other hand, the lineations and striae record a westwards oblique-down-displacement of the northern side of the Salzach–Enns fault (Fig. 3a). These relationships imply that the western portion of the southern side of the Salzach–Enns fault probably exposes a deeper crustal level than the eastern part, in accordance with the regional exhumation pattern.

The latest brittle deformation along the Salzach–Enns fault zone resulted in formation of prominent sets of ca. N-trending conjugate joints without any marker of movement (D_6; Fig. 7). There is no evidence for any structure younger than this set of conjugate joints in the area. The dihedral angle of these joints is about 30°. The acute angle bisectrix is vertical and indicates a vertical orientation of maximum principal stress axis (Fig. 7). Apparently, the latest stage uplift, which is still active (Senftl and Exner, 1973), is responsible for the formation of these conjugate joints.

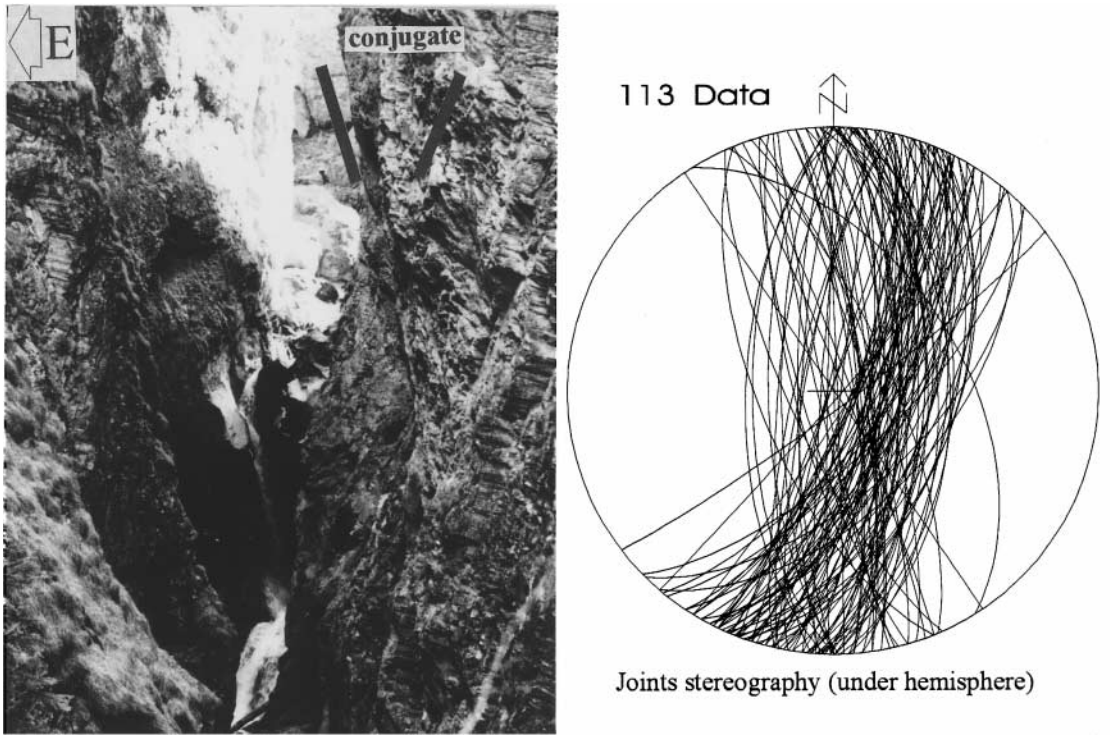

Fig. 7. Representative examples of conjugate joints with vertical acute angles of about 30°. Right diagram shows stereographic projection of conjugate joints within this exposure.

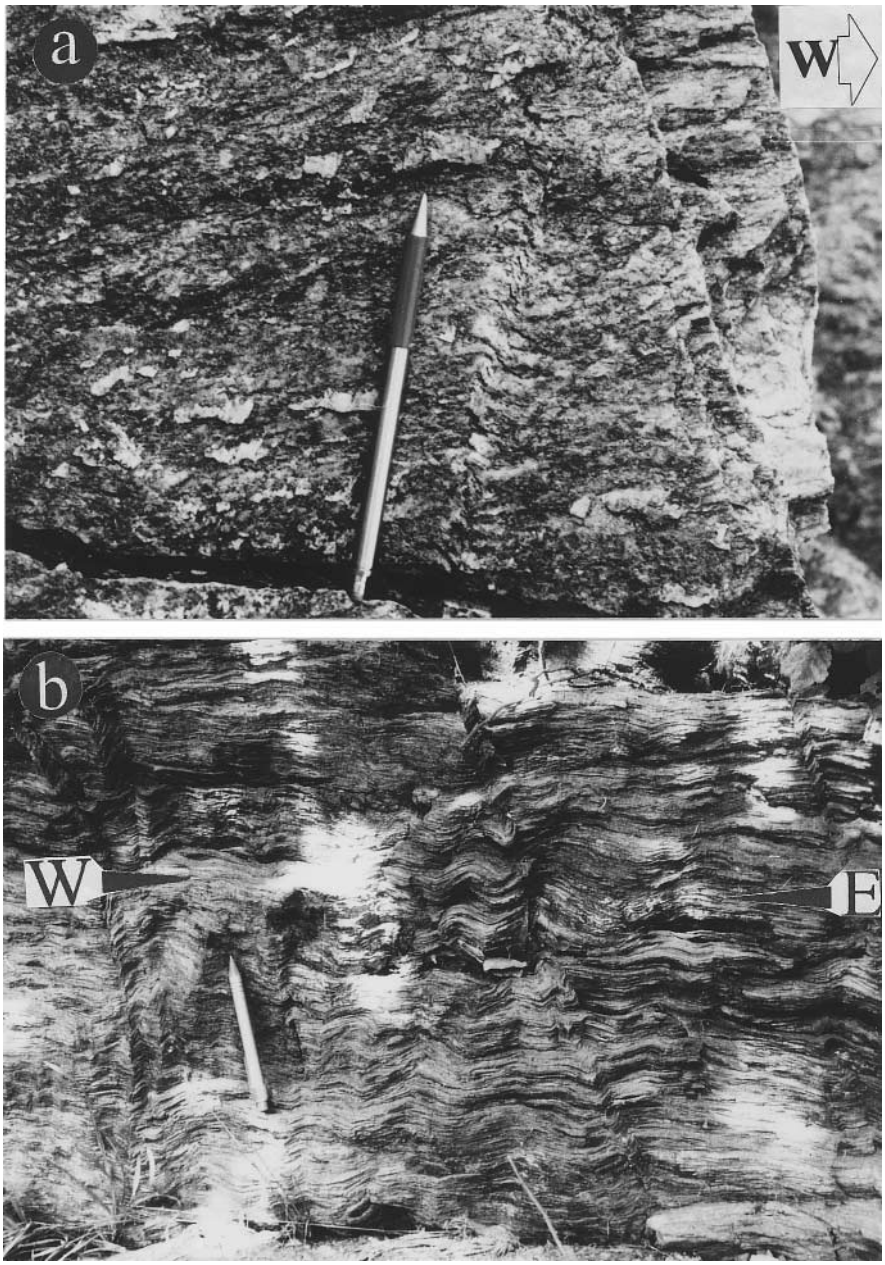

Fig. 8. (a) Steeply plunging kink folds showing sinistral slip of steep sequences with E–W strike. The kinks are overprinted by dip-slip striations (S of Höllmoos). (b) Chevron folds with vertical fold axes in Penninic cover schists of the fault zone document horizontal E–W shortening during latest deformational stage of the Salzach–Enns fault (Mayereinöden).

Kinks

Two types of kinks on centimetre-scale occur within and adjacent to the Salzach–Enns fault zone. Kinks related to sinistral strike-slip affect steeply dipping carbonate phyllites (Fig. 8a). They form where the schistosity is parallel to sinistral shear planes of the fault, similar to those produced by experiments of Tchalenko (1968). The other type of kinks occurs as vertical N–S trending bands in relatively gently dipping rocks. They are found only locally in the area adjacent to the western termination of the Salzach–Enns fault zone (Fig. 8b). We did not find any later deformation of the kinks, but some dextral slickensides closely parallel to the strike of the Salzach–Enns fault are cut by the kinks. These kinks are likely related with the deformation at the western termination of the Salzach–Enns fault and attributed to late-stage E–W shortening which accommodated dextral strike-slip shearing towards the east within the Salzach–Enns fault zone.

PALEOSTRESS PATTERNS

Polyphase paleostress patterns along the Salzach–Enns fault zone were investigated in 40 stations with well exposed rocks, each of which is characterized by relatively homogeneous stress and strain. More than 2000 data sets on the orientations of slickensides and

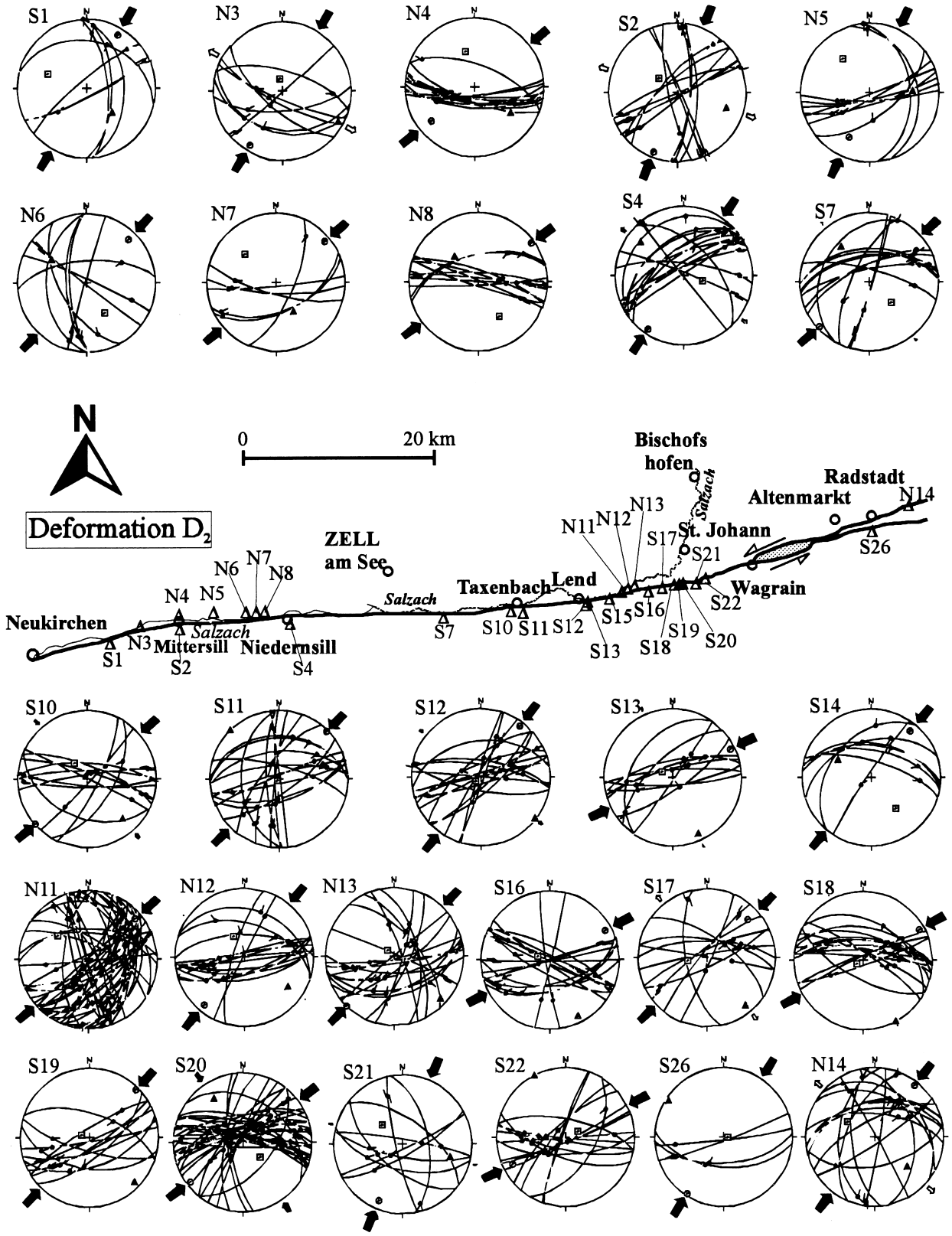

Fig. 9. Orientation data of slickensides and striations and tensor diagrams for the first brittle deformation stage (D_2) along the Salzach–Enns fault zone: Black arrows indicate compression directions. In the tensor graphs, circles represent maximum principal stresses, triangles intermediate principal stresses and squares minimum principal stresses. Little blank triangles locate stations for measurements.

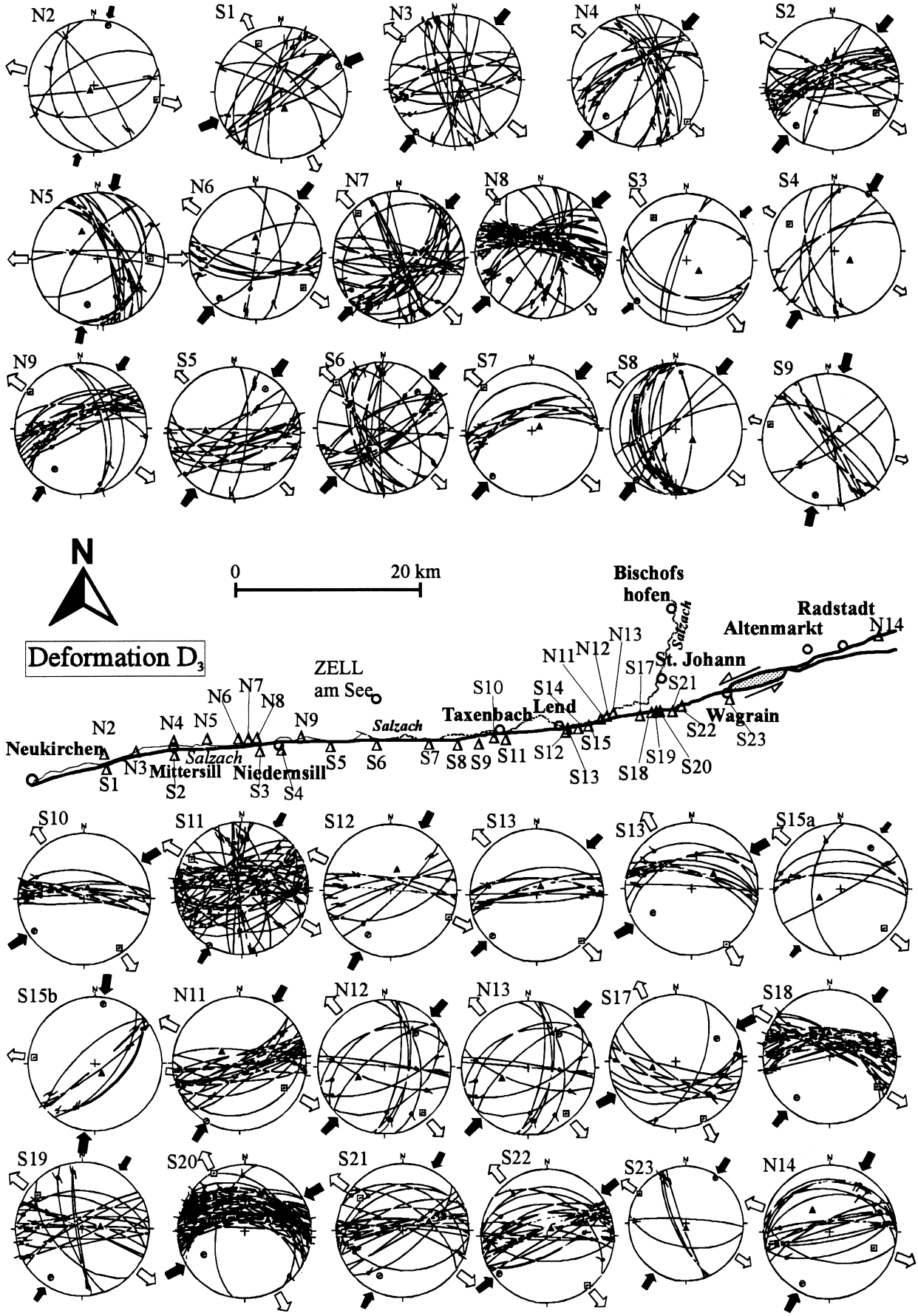

Fig. 10. Orientation data of slickensides and striations and tensor diagrams for D_3 deformation along the Salzach–Enns fault zone. Data presentation as in Fig. 9.

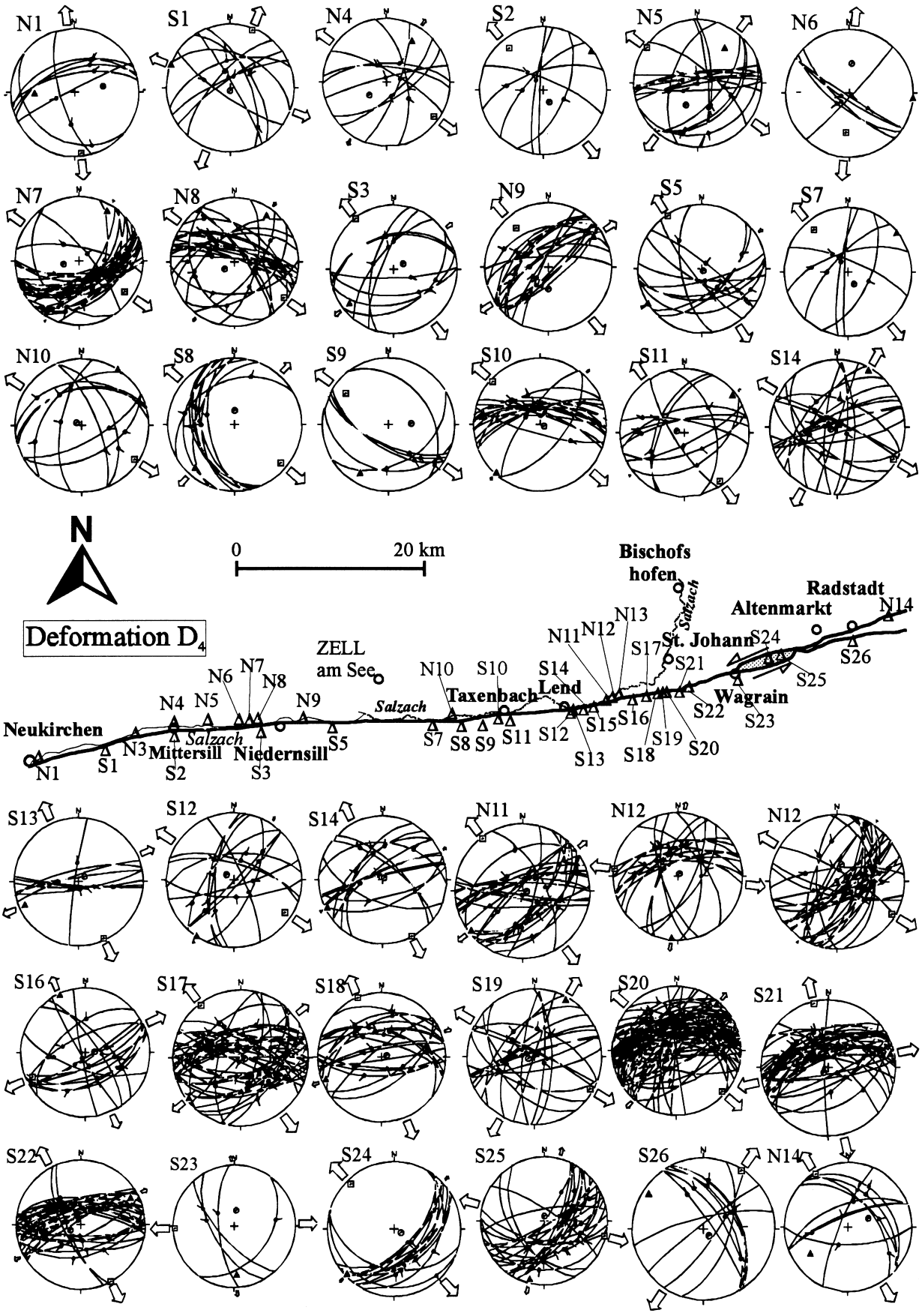

Fig. 11. Orientation data of slickensides and striations and tensor diagrams for D_4 deformation along the Salzach–Enns fault zone. For explanation see Fig. 9.

striations were collected. Overprint criteria in the field were used as a primary source of subdivision. The TENSOR-program (Stapel and Moeys, 1994) was taken as an auxiliary means to divide the data into groups, each of them corresponding to a certain deformation stage. Combined with the evidence for separating deformation stages in the field, four brittle stages of kinematics following ductile D_1 deformation of the Salzach–Enns fault have been found as follows:

(a) The earliest brittle phase (D_2) exhibits a group of compressive or strike-slip compressive tensors (Fig. 9) pertinent to the majority of striations with sinistral shear along ENE-trending slickensides with a reverse component of slip and the minority with dextral shear along NNE-trending planes. These tensors are characterized by a ca. NE 45°–SW 225° trending, subhorizontal maximum principal stress (σ_1) and subvertical minimum principal stress (σ_3) (Fig. 9). D_2 kinematics mainly reflects NE–SW oblique compression in the early deformation period of the Salzach–Enns fault.

(b) Subsequent D_3 kinematics is responsible for a group of pure strike-slip tensors ascribed to prominent E–W sinistral shearing and minor N–S dextral shearing (Fig. 10). The group tensors have a NNE 30°–SSW 210° subhorizontal maximum principal stress σ_1 and a subhorizontal minimum principal stress σ_3 (Fig. 10). With regards to D_2 orientation, σ_1 rotated by ca. 15° in a counter-clockwise sense from D_2 to D_3. The D_3 represents the main deformation period of the fault and accommodated the predominance of sinistral strike-slip displacement in a pure strike-slip.

(c) D_4 kinematics corresponds to a group of pure or radial extensive tensors (Fig. 11) related to the steeply plunging, normal slip striations. The group tensors show a subvertical σ_1 and a predominant subhorizontal NW–SE σ_3 orientation. These steeply plunging, normal-slip striae overprinted the sinistral shearing striae of D_2 and D_3 faulting (Fig. 3e & f), corroborating that the extensive event responsible for steeply plunging striations is subsequent to D_3 pure strike-slip faulting. These structures are the earliest slickensides found in Miocene rocks of the Wagrain basin (Fig. 12).

(d) D_5 kinematics is represented by a group of compressive or strike-slip tensors with subhorizontal NNW340°–SSE160° σ_1 orientation (Fig. 13). The group tensors resulted in both close E–W dextral-shear striations and N–S sinistral-shear striae which locally overprinted earlier steep-plunging normal-slip striations. With regard to the third stage tensors, σ_1 orientations rotated about 50° in counter-clockwise sense from NE 30° to NW 340° (Figs 10 & 13).

(e) D_6 is recorded, as described in previous section, by prominent conjugate joints with vertical acute angle bisectors (Fig. 7), in accordance with present-day uplift of the Alps. This last stage uplift has no relationship with the action of the Salzach–Enns fault.

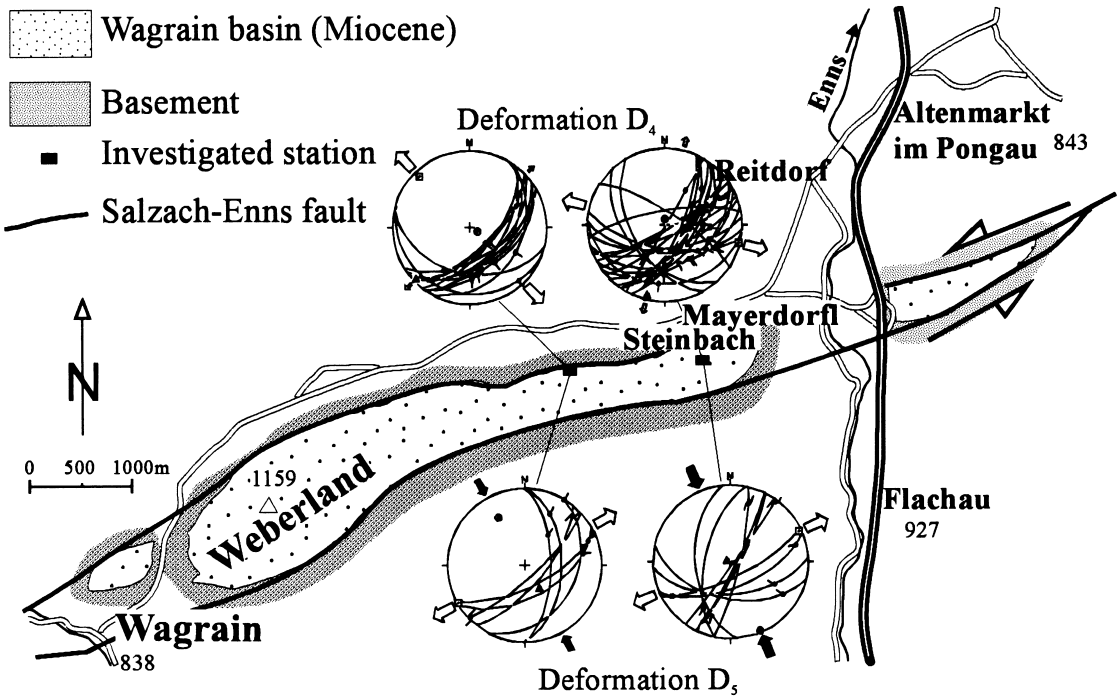

Fig. 12. Simplified map of the Wagrain Lower Miocene sedimentary basin in the left-stepping bend of the strike of the Salzach–Enns fault. Paleostress tensor diagrams yielded by data of fault slip data in this sedimentary area shown. Upper two tensor diagrams show NW–SE extension and lower two tensor diagrams show pure dextral strike-slip stresses along the ENE trending faults.

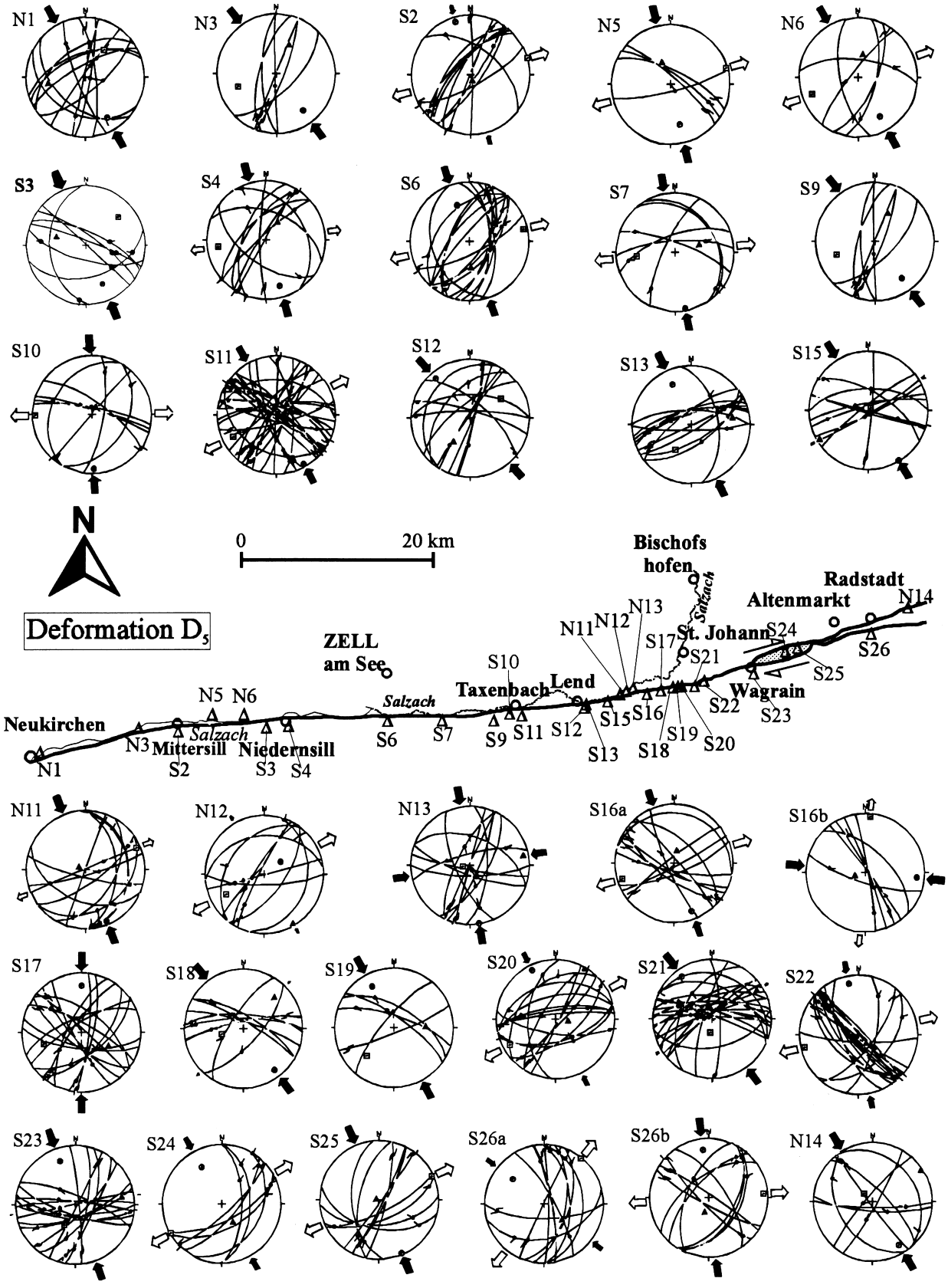

Fig. 13. Orientation data of slickensides and striations and tensor diagrams yielded by the data during D_5 deformation along the Salzach–Enns fault zone. For explanation see Fig. 9.

DISCUSSION

Some aspects of strike-slip faults related to transpression have been well studied, such as effects on the variety of strike-slip fault geometries (Woodcock, 1986; Sylvester, 1988), strain partitioning (e.g. Oldow, 1990; Sanderson and Marchini, 1984) and displacement-partitioning in transpressional orogens (Tikoff and Teyssier, 1994). The Salzach–Enns fault displays some features, such as the transition from ductile to brittle deformation along strike and on vertical sections and the kinematic relationship between horizontal and vertical displacements.

Implications from rheology at different depths along the fault zone

The Salzach–Enns fault zone underwent a transition from early ductile to late brittle deformation. Slickensides and striations are mainly associated with drag structures (Fig. 5d) in western parts, while tensile bridge structures and cataclastic structures (Fig. 8c) dominate in the east. This indicates a differential exhumation along strike of the fault, with maximum uplift in the west. Also, brittle structures such as slickensides and striations and ductile deformation features such as lineations and calcite mylonites occasionally concur within the Salzach–Enns fault zone: brittle dextral and ductile sinistral shears jointly constitute a set of conjugate shear patterns (Fig. 5e). This agrees with observations in western Tauern Window where brittle deformation developed at a depth of ca. 10 km (Selverstone *et al.*, 1995). Furthermore, the progressive structural transition from lineations to striations (Fig. 3d) shows a successive transition from ductile to brittle structures, both for sinistral strike-slip along the fault zone (Fig. 15). These relationships show that ductile shortening orthogonal to the fault surface at deep levels (as expressed, e.g. by calcite mylonites which formed after cleavage lineations and transected folds) is concurrent with brittle sinistral strike-slip with a dip-slip component at shallow structural levels. Thus, the brittle–ductile deformation within the Salzach–Enns fault zone not only represents a continuous succession of deformation in time, but also reflects a continuous vertical section formed during the same event.

Implications for strike-slip fault kinematics

Displacement vectors in the brittle to the ductile domain differ and this indicates a difference in strike-slip fault kinematics from shallow levels to deeper levels during D_3 sinistral-slip faulting.

Striations that represent deformation at shallow levels occur in two different directions of movement, both subhorizontal displacement and steep-plunge normal slip (Fig. 3f). W-plunging sinistral-shear striations indicate that the dip-slip component during sinistral strike-slip faulting contributed to the exhumation of Penninic units of the Tauern Window in respect to the northerly adjacent Austroalpine block. In contrast, ductile shear sense indicators and the fabric of calcite mylonites only express gently W-plunging shear and subhorizontal shortening at deeper levels (Fig. 6). There is no evidence of major late-stage ductile dip-slip displacement. The fabrics of the calcite mylonites exhibit significant pure shear deformation components (Fig. 6), which demonstrate a coaxial flattening component at deeper structural levels. The coaxial flattening resulted in shortening perpendicular to the fault zone and stretching parallel to the fault. This is interpreted to accommodate extrusion of material from deeper levels towards the free upper surface. In response to ductile extrusion from deeper levels, the southern side of the Salzach–Enns fault was exhumed along the fault plane to shallower levels ("stretching fault" according to Means, 1989). Therefore, the brittle dip-slip component at shallow levels and ductile coaxial flattening at deeper levels mutually contributed to the exhumation of the Penninic units.

The bulk of brittle structures, i.e. striations and bridge structures (Figs 3d, e & 5f), shows sinistral strike-slip displacement along the Salzach–Enns fault at shallow levels during D_3; the maximum possible displacement is 60 km (Linzer *et al.*, 1997). Ductile deformation structures such as calcite mylonites, however, mainly present pure shear progressive deformation instead of sinistral simple shear at deeper levels. This means that horizontal displacement in the fault zone at shallow structural levels was larger than that at deeper levels during dominant sinistral strike-slip displacement of the Salzach–Enns fault. If this is true, then the translation on the strike-slip fault is not expected to have the same magnitude everywhere. The overall effect is a hinge movement of the fault with a rotation axis at depth in the crust. There are two substantial arguments for this interpretation: (1) Many sinistral shear striations gently curve down to the west (Fig. 3e). This implies that the southern side of the fault supported upwards-directed motion along a curved path; and (2) because of a curved movement trace along the strike of the Salzach–Enns fault the Tauern Window exhumed like a tilting fault block with regard to the northern, Austroalpine block, corresponding to increasing incremental vertical motion from east to west. Figure 14 sketches a kinematic model for the strike-slip fault with the differences in vectors and magnitudes of displacement between shallow and deeper structural levels.

The relevance of post-faulting rotation and of pre-existing faults on the validity of data

The approach of using striations for restoration of paleostress tensors has been applied to separate tectonic phases and achieved a theoretical agreement with

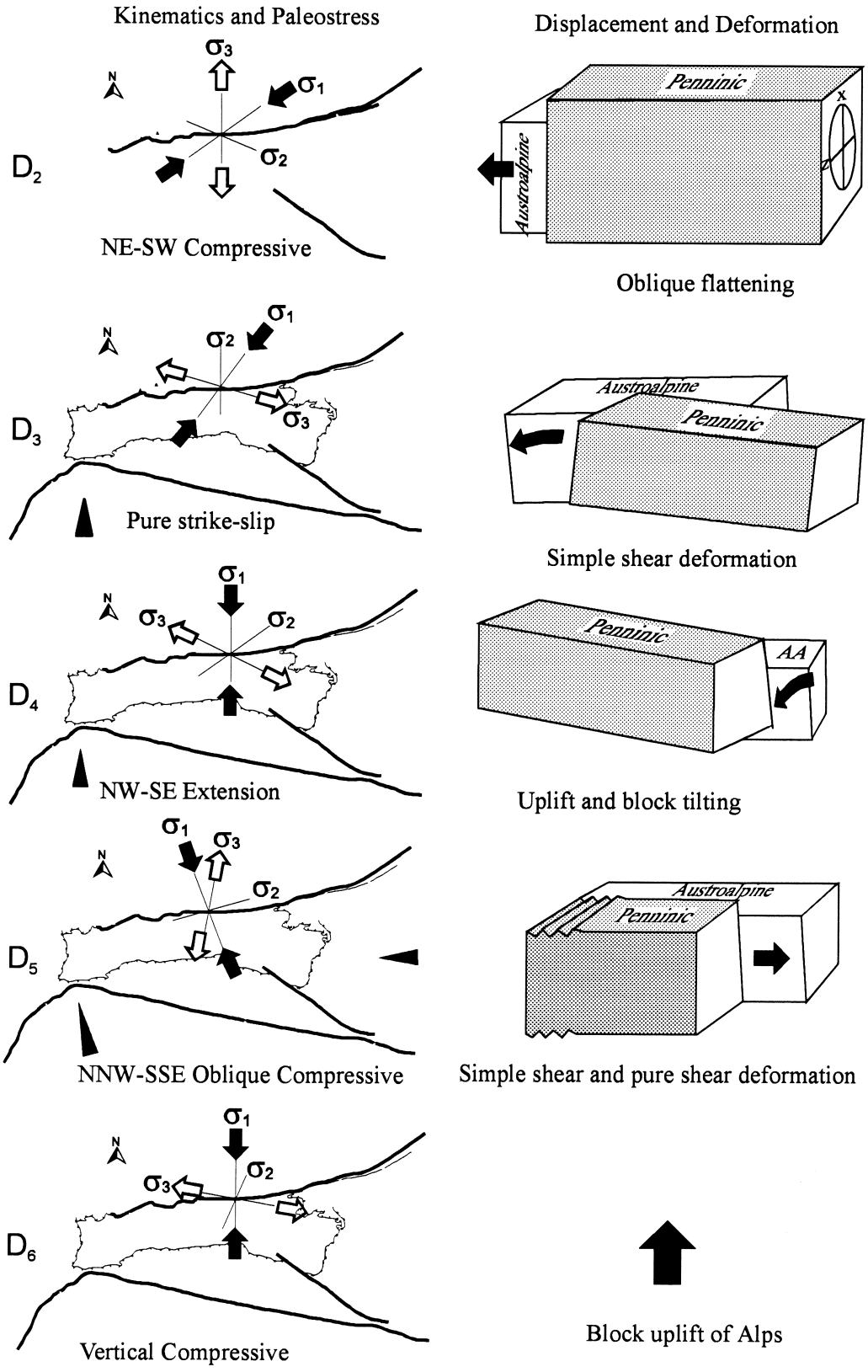

Fig. 15. Schematic model showing the evolution of the Salzach–Enns fault: Blank triangle indicates movement direction of the South Alpine indenter. Thick lines are active faults. Ellipses show resulting strain states. *X* and *Z* show maximum and minimum strain axes, respectively. Square bordered by the fault line is the Tauern Window. For detailed explanation, see text.

independent field criteria (Armijo *et al.*, 1982). Although the approach rests on many assumptions, it remains a practical method for analysis of multiphase paleostress as long as its result is in agreement with independent field observations. Clearly, the presence of post-faulting rotation and pre-existing faults affects the validity of orientation data of striae and slickensides for an analysis of polyphase kinematics (Marrett and Allmendiger, 1990).

With the TENSOR program (Stapel and Moeys, 1994) we searched for reduced stress tensors that give the smallest possible differences between the observed slip direction and the maximum computed shear stress on the given planes (=slip deviation) for a maximum number of faults. The procedure is repeated for incompatible faults. For a low angle of slip deviation (average about 15°) the data for the second stage tensor are consistent with field observations. This suggests that sinistral strike-slip dominated the deformation within the Salzach–Enns fault, and pre-existing fault and post-faulting rotation did not significantly affect these data sets. On the contrary, the fourth and fifth stage tensors show slightly greater slip deviations (average about 20°) and lower axial ratio (about 0.3–0.5). This shows that the pre-existing fault surfaces may control to some extent late faulting. As a result, the striations of the fourth and fifth structural stages in many locations developed on slickensides of the second stage, where a few sets of striae with different plunge directions appear on one slickenside (Fig. 5c & 3f). Still, the value of slip deviations during the fourth and fifth stage actions remains in a permissible range. There is not a marked difference between the second and third stage deformations; both mainly express sinistral strike-slip structures. Therefore, the third stage faulting did not modify the second stage deformations greatly although both had different paleostress fields. This also suggests that sufficient fault-slip data allow to analyse multiphase kinematics. Then the calculation of multiphase tensors with the tensor programs can be expected to separate the tectonic phases of brittle deformation events in regions where extensive information about fault-slip exists.

Structures in the bent segment of the Salzach–Enns fault

The Wagrain sedimentary basin within the bent segment of the Salzach–Enns fault, exposed now between Wagrain and Altenmarkt, sustained brittle deformation associated with the Salzach–Enns fault. Structural investigations and paleostress analysis of two stations within this sedimentary body show steeply plunging striations and dextral slip striations on the fault planes but no sinistral slip striations and defined only the tensors of D_4 and D_5 deformations (Fig. 12). The location of the basin demonstrates that its development is concurrent with formation of the Salzach–Enns fault in the Lower Miocene. A pull-part origin within this releasing bend, attributed to necessity of pure sinistral strike-slip parallel to the general strike of the fault for the left bent segment (Crowell, 1974), is a possible mechanism for the local subsidence. The development of the Salzach–Enns fault concurred also with the E–W extension of the Tauern Window during the Miocene (Selverstone, 1988; Genser and Neubauer, 1989). This case supports the view that sinistral transpression and E–W extension are basic aspects of a model for the exhumation of the Tauern Window during the Tertiary (e.g. Selverstone, 1988; Behrmann, 1988; Genser and Neubauer, 1989; Neubauer and Genser, 1990; Ratschbacher *et al.*, 1991; Genser, 1992; Kurz and Neubauer, 1996).

The kinematics related to the fourth brittle event (D_5)

There are two kinds of distinct deformation features along the Salzach–Enns fault zone that belong to the deformation stage D_5. The kinks that predominate in the west (Fig. 8b) are replaced by dextral shear deformations towards the east. These kinks have vertical kink planes and approximately N trending kink axes. Except for rare conjugate joints in D_6, no other structures have been found to deform them. It appears reasonable that the kinks and the dextral shears formed at a shallow structural level within low temperature conditions and during the last stage NW–SE oblique compression along the Salzach–Enns fault. The kinks are only located to the west of Taxenbach; in the east only the E–W trending dextral shear striations developed. The distribution of these structures indicates that E–W shortening in the W was transferred towards east into dextral shearing along the fault zone. We therefore suggest that it was caused by the late northwestward motion of the South Alpine indenter and an E–W compression. The E–W compression probably originated from far-field effects of Late Miocene subduction in the Eastern Carpathians (Peresson and Decker, 1997), where after cessation of west-directed subduction of the European plate below the Eastern Carpathians, continued convergence induced westward transmission of E–W directed compressive stresses. A NW–SE compressive stress field along the Salzach–Enns fault zone was established by superposition of E–W compression and the continued northward movement of the South Alpine indenter. This palaeostress field induced a change from sinistral strike-slip displacement to dextral strike-slip along the Salzach–Enns fault zone. The westward replacement of dextral strike-slip faulting by kinks indicates that dextral strike-slip faulting was transferred to orthogonal shortening in the compressive sector of its termination. Also, the transmission of E–W directed compressive stresses was likely reduced westwards and terminated in the western section of the fault zone.

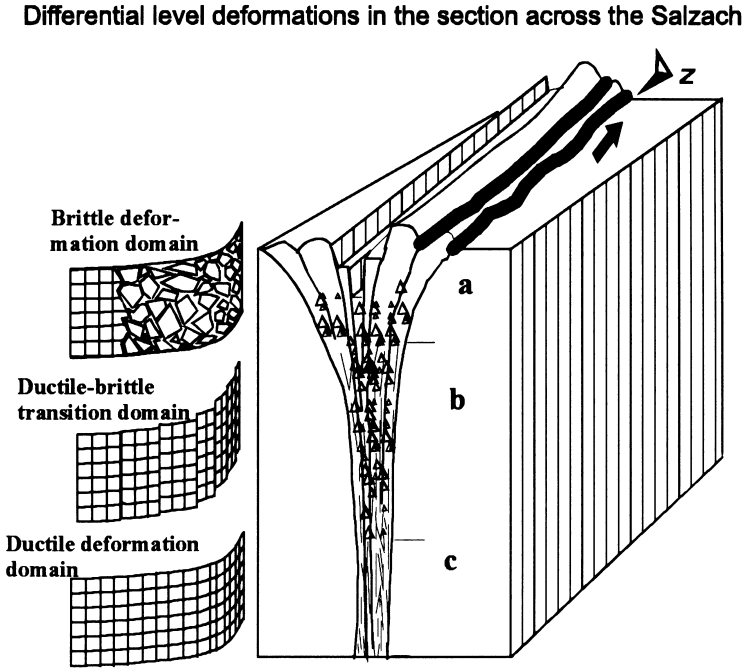

Fig. 15. Schematic cross section of the Salzach–Enns fault showing deformations at different structural levels. (a) Brittle deformation domain; (b) ductile–brittle transition domain; (c) ductile deformation domain.

The sequence of multi-stage kinematics of the Salzach–Enns fault zone

The development of the Salzach–Enns fault was a continuous process, although divided into a succession of six deformation stages (Fig. 14). The movement of southern part of the South-Alpine unit towards the north (e.g. Ratschbacher *et al*., 1991; Neubauer, 1994; Kurz *et al*., 1994) induced NE–SW compression and triggered the Salzach–Enns fault along the boundary of Penninic and Austroalpine units, which acted as a boundary of two tectonic units with different temperature-controlled rheologies. Compression oblique to the Salzach–Enns fault produced sinistral transpression, recorded by transected folds and crenulation lineations intersected by the fold hinge line in a clockwise sense during D_1 deformation stage kinematics (Fig. 4). The initial brittle deformation stage D_2 is represented by a vertical minimum principal stress axis and horizontal maximum principal stress axis, and the overall deformational type is of pure-shear dominated transpression (Tikoff and Teyssier, 1994). The pure-shear dominated transpression was gradually replaced by wrench-dominated transpression as the development of the Salzach–Enns fault zone led to stress release. Then a NE–SW compressive paleostress field was set up with a vertical intermediate principal stress axis (Fig. 15). Subsequent movement of the South Alpine indenter towards the north further enhanced compression (Fig. 15). The wrench-dominated transpression accommodated a large amount of subhorizontal sinistral shear displacement documented by E–W striations at shallow structural levels (e.g. Fig. 3e & f) and calcite mylonite at deeper structural levels (e.g. Figs 5a,b & 15). Simultaneously with or following the wrench-dominated transpression the exhumation of the southern side of the fault, constituted by Penninic units, is documented by steep-plunging striae which yield a paleostress state with a vertical maximum principal stress axis. Late Miocene E–W compression resulted from westward transmission of E–W directed compressive stresses in the Eastern Carpathian region and sustained movement of the South Alpine indenter towards north induced a NW–SE compressive stress field within the Salzach–Enns fault zone (Fig. 14), which reversed the sinistral strike-slip faulting. The multi-stage kinematic evolution of the Salzach–Enns faulting during Tertiary mentioned above partly corroborates earlier investigations in other sectors of the Eastern Alps (e.g. Kurz *et al*., 1994; Neubauer, 1994; Polinski and Eisbacher, 1992; Nemes *et al*., 1995; Linzer *et al*., 1997; Peresson and Decker, 1997).

Acknowledgements—This study was funded of the Austrian Research Foundation (grant no. 9918). We thank Johann Genser and Walter Kurz for invaluable advice on the calculation method of paleostress and many stimulating discussions about microstructures. We gratefully acknowledge reviews and remarks to an earlier version of the manuscript by Lothar Ratschbacher, Jane Selverstone and Cees Passchier. We thank Franz Nemes, Robert Handler, Gerhard Xi Amann, Hans Steyrer, Joachim Schweigl, Ewald Hejl and Gertrude Friedl for their assistance.

REFERENCES

Angelier, J. (1979) Determination of the mean principal direction of stresses for a given fault population. *Tectonophysics* **56,** T17–T26.

Armijo, R., Carey, E. and Cisternas, A. (1982) The inverse problem in microtectonics and the separation of tectonic phases. *Tectonophysics* **82,** 145–160.

Behrmann, J. H. (1988) Crustal-scale extension in a convergent orogen: the Sterzing–Steinach mylonite zone in the Eastern Alps. *Geodinamica Acta* **2,** 63–73.

Behrmann, J. H. and Frisch, W. (1990) Sinistral ductile shearing associated with metamorphic decompression in the Tauern Window, Eastern Alps. *Jahrbuch der Geologischen Bundesanstalt* **133,** 135–146.

Bickle, M. J. and Hawkesworth, C. J. (1978) Deformation phases and tectonic history of the eastern Alps. *Geological Society of America Bulletin* **89,** 293–306.

Burkhard, M. (1993) Calcite twins, their geometry, appearance and significance as stress–strain markers and indicators of tectonic regime: a review. *Journal of Structural Geology* **15,** 351–368.

Busch, J. P. and van der Pluijm, B. A. (1995) Calcite textures, microstructures and rheological properties of marble mylonites in the Bancroft shear zone, Ontario, Canada. *Journal of Structural Geology* **17,** 677–688.

Coney, P. J. (1980) Cordilleran metamorphic core complexes: an overview. *Geological Society of America Memoir* **153,** 7–35.

Crowell, J. C. (1974). Sedimentation along the San Andreas Fault, California. In *Modern and Ancient Geocynclinal Sedimentation* eds R. H. Dott Jr and R. H. Shaver. Society of Economic Paleontologists and Mineralogists Special Publication, **19,** 292–303.

Dewey, J. F. (1988) Extensional collapse of orogens. *Tectonics* **7,** 1123–1139.

Droop, G. T. R. (1985) Alpine metamorphism in the south-east Tauern Window, Austria: 1. *P–T* variation in space and time. *Journal of Metamorphic Geology* **3,** 371–402.

Exner, C. (1996) Leitgesteine und Tektonik in Phylliten bei Wagrain und Radstadt (Land Salzburg). *Jahrbuch der Geologischen Bundesanstalt* **139,** 155–190.

Frisch, W. (1979) Tectonic progradation and plate tectonic evolution of the Alps. *Tectonophysics* **60,** 121–139.

Frisch, W. (1980) Post-Hercynian formations of western Tauern window: Sedimentological features, depositional environment, and age. *Mitteilungen der Österreichischen Geologischen Gesellschaft* **71/72,** 49–63.

Gamond, J. F. (1983) Displacement features associated with fault zones: a comparison between observed and experimental models. *Journal of Structural Geology* **5,** 33–45.

Gamond, J. F. (1987) Bridge structures as sense of displacement in brittle fault zones. *Journal of Structural Geology* **9,** 609–620.

Genser, J. (1992) Struktur-, Gefüge- und Metamorphoseentwicklung einer kollisionalen Plattengrenze: Das Beispiel des Tauernostrandes (Kärnten/Österreich). Ph.D. thesis, University of Graz.

Genser, J. and Neubauer, F. (1989) Low angle normal faults at the eastern margin of the Tauern Window (Eastern Alps). *Mitteilungen der Österreichischen Geologischen Gesellschaft* **81,** 233–243.

Genser, J., Van Wees, J. D., Cloetingh, S. and Neubauer, F. (1996) Eastern Alpine tectono-metamorphic evolution: Constraints from two-dimensional *P–T–t* modeling. *Tectonics* **15,** 584–604.

Hanmer, S. and Passchier, C. (1991) Shear sense indicators: a review. *Geological Survey of Canada Paper* **90-17,** 1–72.

Hobbs, B. E., Means, W. D. and Williams, P. E. (1976) *An Outline of Structural Geology*. 571 p. Wiley and Sons, New York.

Holdsworth, R. E. and Strachan, R. A. (1991) Interlinked system of ductile strike slip and thrusting formed by Caledonian sinistral transpression in northeastern Greenland. *Geology* **19,** 510–513.

Ichikawa, K. (1980) Geohistory of the Median Tectonic Line of southwestern Japan. *Memoir of the Geological Society of Japan* **18,** 187–212.

Kruhl, J. H. (1993) The *P–T–d* development at the basement-cover boundary in the north-eastern Tauern window (Eastern Alps): Alpine continental collision. *Journal of Metamorphic Geology* **11,** 31–47.

Kurz, W., Neubauer, F., Genser, H. and Horner, H. (1994) Sequence of Tertiary brittle deformations in the eastern Tauern Window (Eastern Alps). *Mitteilungen der Österreichischen Geologischen Gesellschaft* **86,** 573–605.

Kurz, W. and Neubauer, F. (1996) Deformation partitioning during updoming of the Sonnblick area in the Tauern Window (Eastern Alps, Austria). *Journal of Structural Geology* **18,** 1327–1343.

Kurz, W., Neubauer, F. and Genser, H. (1996) Kinematics of Penninic nappes (Glockner Nappe and basement-cover nappes) in the Tauern Window (Eastern Alps, Austria) during subduction and Penninic–Austroalpine collision. *Eclogae Geologicae Helvetiae* **89,** 573–605.

Lammerer, B. (1988) Thrust-regime and transpression-regime tectonics in the Tauern Window (Eastern Alps). *Geologische Rundschau* **77,** 143–156.

Linzer, H.-G., Moser, F., Nemes, F., Ratschbacher, L. and Sperner, B. (1997) Build-up and dismembering of the eastern Northern Calcareous Alps. *Tectonophysics* **272,** 97–124.

Lister, G. S. and Williams, P. F. (1979) Fabric development in shear zones: theoretical controls and observed phenomena. *Journal of Structural Geology* **1,** 283–297.

Lister, G. S. and Davis, G. A. (1989) The origin of metamorphic core complexes and detachment faults formed during Tertiary continental extension in the Colorado River region, U.S.A. *Journal of Structural Geology* **11,** 65–94.

Malavielle, J. (1987) Kinematics of compressional and extensional ductile shearing deformation in a metamorphic core complex of the northeastern Basin and Range. *Journal of Structural Geology* **9,** 541–554.

Manning, A. H. and Bartley, J. M. (1994) Postmylonitic deformation in the Raft River metamorphic core complex, northwestern Utah: evidence of a rolling hinge. *Tectonics* **13,** 596–612.

Marrett, R. and Allmendinger, R. W. (1990) Kinematic analysis of fault slip data. *Journal of Structural Geology* **12,** 973–986.

Means, W. D. (1989) Stretching faults. *Geology* **17,** 893–896.

Nemes, F., Pavlik, W. and Moser, M. (1995) Geologie und Tektonik im Salzatal (Steiermark)—Kinematik und Paläospannungen entlang des Ennstal–Mariazell–Blattverschiebungssystems in den Nördlichen Kalkalpen. *Jahrbuch der Geologischen Bundesanstalt* **138,** 349–367.

Neubauer, F. (1994) Kontinentkollision in den Ostalpen. *Geowissenschaften* **12,** 136–140.

Neubauer, F. and Genser, J. (1990) Architektur und Kinematik der östlichen Zentralalpen—eine Übersicht. *Mitteilungen des naturwissenschaftlichen Vereins der Steiermark* **120,** 203–219.

Neubauer, F., Dallmeyer, R. D., Dunkl, I. and Schirnik, D. (1995) Late Cretaceous exhumation of the metamorphic Gleinalm dome, Eastern Alps: Kinematics, cooling history and sedimentary response in a sinistral wrench corridor. *Tectonophysics* **242,** 79–89.

Norris, D. K. and Barron, K. (1968) Structural analysis of features on natural and artificial faults. *Proceedings of the Conference on Research in Tectonics, Ottawa*, pp. 136–174.

Oldow, J. S. (1990) Transpression, orogenic float, and lithospheric balance. *Geology* **18,** 991–994.

Peresson, H. and Decker, K. (1997) Far-field effects of Late Miocene subduction in the Eastern Carpathians: E–W compression and inversion of structures in the Alpine–Carpathian–Pannonian region. *Tectonics* **16,** 38–56.

Peltzer, G., Tapponnier, P., Zhang, Z. and Xu, Z. (1985) Neogene and Quaternary faulting in and along the Qinling Shan. *Nature* **317,** 500–505.

Petit, J. P. (1987) Criteria for the sense of movement on fault surfaces in brittle rocks. *Journal of Structural Geology* **9,** 597–608.

Platt, J. P. (1993) Exhumation of high-pressure rocks: a review of concepts and processes. *Terra Nova* **5,** 119–133.

Polinski, R. K. and Eisbacher, H. (1992) Deformation partitioning during polyphase oblique convergence in the Karawanken Mountains, southeastern Alps. *Journal of Structural Geology* **14,** 1203–1213.

Ramsay, J. G. and Graham, R. H. (1970) Strain variations in shear belts. *Canadian Journal of Earth Sciences* **7,** 786–813.

Ramsay, J. G. and Huber, M. (1987) *Modern Structural Geology. Volume 2: Folds and Fractures*, pp. xii + 307–700. Academic Press, London.

Ratschbacher, L., Frisch, W., Neubauer, F., Schmid, S. M. and Neugebauer, J. (1989) Extension in compressional orogenic belts: The eastern Alps. *Geology* **17,** 404–407.

Ratschbacher, L., Frisch, W., Linzer, H. G. and Merle, O. (1991) Lateral extrusion in the eastern Alps, Part 2: Structural analysis. *Tectonics* **10,** 257–271.

Rutter, E. H., Casey, M. and Burlini, L. (1994) Preferred crystallographic orientation development during the plastic and superplastic flow of calcite rocks. *Journal of Structural Geology* **16,** 1431–1446..

Sanderson, D. J. and Marchini, W. R. D. (1984) Transpression. *Journal of Structural Geology* **6,** 449–458.

Schmid, S. M., Paterson, M. S. and Boland, J. N. (1980) High temperature flow and dynamic recrystallisation in Carrara marble. *Tectonophysics* **65,** 245–280.

Schmid, S. M., Panozzo, R. and Bauer, S. (1987) Simple shear experiments on calcite rocks: rheology and microfabrics. *Journal of Structural Geology* **9,** 747–778.

Selverstone, J. (1985) Petrologic constraints on imbrication, metamorphism, and uplift in the SW Tauern Window, Eastern Alps. *Tectonics* **4,** 687–704.

Selverstone, J. (1988) Evidence for east–west crustal extension in the Eastern Alps: implications for the unroofing history of the Tauern Window. *Tectonics* **7,** 87–105.

Selverstone, J., Axen, G. J. and Bartley, J. M. (1995) Fluid inclusion constraints on the kinematics of footwall uplift beneath the Brenner Line normal fault, eastern Alps. *Tectonics* **14,** 264–278.

Senftl, E. and Exner, Ch. (1973) Rezente Hebung der Hohen Tauern und geologische interpretation. *Verhandlungen der Geologischen Bundesanstal* **1973,** 209–234.

Simpson, C. and Schmid, S. M. (1983) An evaluation of criteria to deduce the sense of movements in sheared rocks. *Geological Society of America Bulletin* **94,** 1281–1288.

Soper, N. J. (1986) Geometry of anastomosing solution cleavage in transpression zones. *Journal of Structural Geology* **8,** 937–940.

Soper, N. J. and Hutton, D. H. W. (1984) Late Caledonian sinistral displacements in Britain: implications for three-plate collision model. *Tectonics* **3,** 781–794.

Stapel, G. and Moeys, R. (1994) *Manual for the D. Delvaux Tensor program.* Free University, Amsterdam.

Staufenberg, H. (1987) Apatite fission-track evidence for postmetamorphic uplift and cooling history of the eastern Tauern Window and the surrounding Austroalpine (Central Eastern Alps, Austria). *Jahrbuch der Geologischen Bundesanstalt* **130,** 571–586.

Stringer, P. and Treagus, S. H. (1980) Non-axial planar S_1 in the Hawick Rocks of the Galloway area, Southern Uplands, Scotland. *Journal of Structural Geology* **2,** 317–331.

Suggate, R. P. (1963) The Alpine Fault. *Transactions Royal Society New Zealand Geology* **2,** 105–129.

Sylvester, A. G. (1988) Strike-slip faults. *Geological Society of America Bulletin* **100,** 1666–1703.

Tchalenko, J. S. (1968) The evolution of kink-bands and the development of compression textures in sheared clays. *Tectonophysics* **6,** 159–174.

Tikoff, B. and Teyssier, C. (1994) Strain modeling of displacement-field partitioning in transpressional orogens. *Journal of Structural Geology* **16,** 1575–1588.

Treagus, S. H. and Treagus, J. E. (1992) Transected folds and transpression: How are they associated? *Journal of Structural Geology* **14,** 361–367.

Trauth, F. (1925) Geologie der nördlichen Radstädter Tauern and ihres Vorlandes, I, II. *Denkschrift der Akademie der Wissenschaften Wien, mathematisch-naturwissenschaftliche Klasse, 1. Teil* **100,** 101–212.

Weber, L. and Weiss, A. (1983) Bergbaugeschichte und Geologie der Österreichischen Braunkohlenvorkommen. *Archiv für Lagerstättenforschung an der Geologischen Bundesanstalt* **4,** 177–179.

Wenk, H. R., Takeschita, T., Bechler, E., Erskine, B. and Matthies, S. (1987) Pure shear and simple shear calcite textures. Comparison of experimental, theoretical and natural data. *Journal of Structural Geology* **9,** 731–745.

Wenk, H. R. and Christie, J. M. (1991) Comments on the interpretation of deformation textures in rocks. *Journal of Structural Geology* **13,** 1091–1110.

Woodcock, N. H. (1986) The role of strike-slip fault systems at plate boundaries. *Philosophical Transaction, Royal Society of London Series A* **317**(1539), 141–177.

Woodcock, N. H., Awan, M. A., Johnson, T. E., Mackie, A. H. and Smith, R. D. (1988) Acadian tectonics in Wales during Avalonia/Laurentia convergence. *Tectonics* **7,** 483–495.